Molecular Crystals and Liquid Crystals
Publication details, including instructions for authors and subscription information:
http://www.tandfonline.com/loi/gmcl20

The Anchoring Strength of Liquid Crystals on Polyimide Surfaces Treated by a Direct-Current Ion Beam Sputter

Chao-Yu Tai [a], Hsin-Ying Wu [a], Meng-Chiou Huang [a b] & Ru-Pin Pan [a]
[a] Department of Electrophysics, National Chiao Tung University, Hsinchu, Taiwan
[b] Institute of Atomic and Molecular Sciences Academia Sinica, Taipei, Taiwan
Published online: 16 Jun 2011.

To cite this article: Chao-Yu Tai, Hsin-Ying Wu, Meng-Chiou Huang & Ru-Pin Pan (2011) The Anchoring Strength of Liquid Crystals on Polyimide Surfaces Treated by a Direct-Current Ion Beam Sputter, Molecular Crystals and Liquid Crystals, 546:1, 116/[1586]-125/[1595], DOI: 10.1080/15421406.2011.571938

To link to this article: http://dx.doi.org/10.1080/15421406.2011.571938

Mol. Cryst. Liq. Cryst., Vol. 546: pp. 116/[1586]–125/[1595], 2011

ISSN: 1542-1406 print/1563-5287 online
DOI: 10.1080/15421406.2011.571938

Taylor & Francis
Taylor & Francis Group

The Anchoring Strength of Liquid Crystals on Polyimide Surfaces Treated by a Direct-Current Ion Beam Sputter

CHAO-YU TAI,[1] HSIN-YING WU,[1]
MENG-CHIOU HUANG,[1,2] AND RU-PIN PAN[1]

[1]Department of Electrophysics, National Chiao Tung University, Hsinchu, Taiwan
[2]Institute of Atomic and Molecular Sciences Academia Sinica, Taipei, Taiwan

In this work we report the alignment property of nematic liquid crystal with variable pretilt angle on surfaces treated by argon plasma. The scanning electron microscope (SEM) image indicates that nanoparticles are deposited on treated PI film. Groove-like aggregating structures are observed and the direction of aggregate tends to parallel to the ion beam direction. X-ray photoelectron spectroscopic (XPS) analysis confirms that γ-Fe_2O_3 nanoparticles were deposited on the surface of polyimide (PI) films. We also deduce that the maghemite is the main factor determining the pretilt angle while a competition exists between the homogeneous and homeotropic alignments.

Keywords Anchoring strength; ion beam; nanoparticles; polyimide films; pretilt angle; surface alignment

1. Introduction

The alignment film such as polyimide (PI) is commonly used to orient liquid crystal molecules in the liquid crystal displays (LCDs) and other LC devices. The PI film treated with mechanical rubbing, ion beam irradiation, or photo-alignment has been often used to cause alignment along a particular direction. Currently, the most popular alignment method used in LCDs industries is still the rubbing process which generated parallel grooves of about micron size in favor of LC alignment [1]. Despite its successful, the as-rubbed PI film exhibits some drawbacks such as surface electrostatic charge and leaving debris, which are difficult to maintain uniformity as the substrate size of LCD gets larger rapidly. To avoid these disadvantages, non-contact alignment methods are highly desirable. Photo-alignment is useful for induce uniaxial orientation of LC with linear polarized UV light irradiation [2,3]. Over the past

Address correspondence to Ru-Pin Pan, Department of Electrophysics, National Chiao Tung University, Hsinchu, Taiwan 30010. Tel.: 886-3-5131560; Fax: 886-3-5725230; E-mail: rpchao@mail.nctu.edu.tw

decade, Wu et al. described an approach for controlling pretilt angle of LC using fluorinated copolymer film in a two-step irradiation process [4].

Ion beam alignment has been reported first by the IBM group [5,6]. They have successfully realized ion beam alignment technology by low energy ion bombard an alignment film such as PI or diamond-like carbon (DLC). The homeotropic alignment has also been obtained by using fluorinated diamond-like carbon (FDLC) thin films as the alignment layer [7]. Consequently, homogeneous and homeotropic alignment can be obtained by choosing different ion beam parameters or the concentration of fluorine doped in DLC films [8]. This outstanding ion beam alignment method is potentially useful in LC-based application.

Mainly two possible mechanisms have been proposed in explaining the homogeneous LC alignment in literatures. One is the grooving mechanism proposed by Berreman et al. Parallel microgrooves morphology can be generated by mechanical rubbing on some polymer films, which lead LC molecules to align along the grooves to achieve the lowest elastic strain energy [9]. The other is the surface chemical bonding mechanism such as π-π electron coupling proposed by Stöhr et al. The mechanism of this alignment method was referred to the carbon bonds and rings which are oriented perpendicular to the incident beam are destroyed preferentially over those bonds are parallel to the ion beam direction. The amorphous carbon network exhibits a preferential orientation of its σ bonds parallel and π bonds perpendicular to the beam direction, respectively [5].

In this work, we demonstrate a new method to obtain the LC alignment with adjustable pretilt angle. We use argon plasma beam to treat the surface of PI film and induce high pretilt angles. Simultaneously, maghemite, γ-Fe_2O_3, nanoparticles are deposited on PI film. Depending on the argon plasma beam treating conditions, the variable pretilt angle is achieved. We have also measured the polar anchoring strength and azimuthal anchoring strength of the LC molecules on the plasma-treated PI surface such that the competition between maghemite nanoparticles and polyimide can be understood.

2. Experimental Methods

A direct-current ion-coater (IB-3 Eiko engineering co., Tokyo, Japan) has been used for ion coating on substrate that was coated with PI film. Ion sputtering is a phenomenon in which ions or high-energy particles strike a target electrode, causing emission of atoms from the electrode. Sputtering occurs in a cathode glow discharge region near the lower electrode in a relatively low-vacuum chamber. The diameters of the upper and lower electrode in our system are 50 mm and 52 mm, respectively, and the spacing between the stainless steel electrodes is 30 mm. The chamber is pumped down to a base pressure of 30 mTorr. Argon was used as the working gas in the chamber. The pressure of the chamber is adjusted to keep the current density stable. The ion energy was controlled by the anode potential that was varied within the range $0 \sim 1400$ V. The incident angle, the current density and dc bias between the electrodes are fixed at 60°, 255 $\mu A/cm^2$ and 560 V, respectively. The treating time is varied in this research.

A pair of substrates of $20 \times 10\,mm^2$ is placed on the lower electrode in the ion beam chamber. The substrate is indium-tin-oxide (ITO) coated glass with SE-130B (from Nissan Chemical Industries) PI film on top. The PI is spin coated on the ITO glass, pre-baked at 80°C for 10 min, and cured at 170°C for 1 hour. Anti-pallel

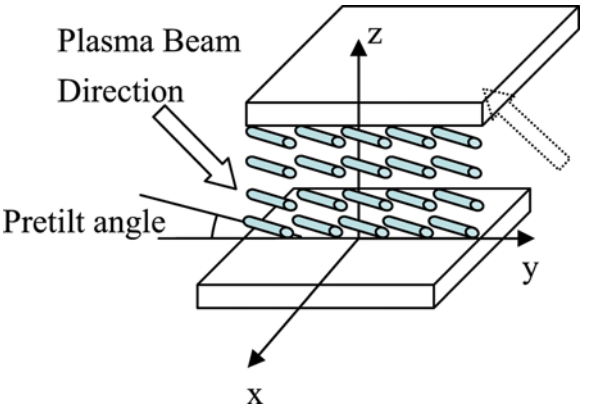

Figure 1. Geometry of the anti-parallel LC cell. (Figure appears in color online.)

empty cell is assembled with these two ion-beam treated substrates and a 23 μm thick Mylar spacer. Nematic LC 4′-n-pentyl-4-cyanobiphenyl (5CB, Merck) in isostropic phase is filled into the empty cell. The pretilt angle of liquid crystal cells are measured by the crystal rotation method. The geometry of the cell is illustrated in Figure 1.

To study the alignment mechanism and control the pretilt angle, it is important to understand the interaction between plasma beam and polyimide. The pretilt angle of liquid crystal cells are measured by the crystal rotation method [10]. The surface morphologies and roughness of the plasma-treated PI film are characterized by using scanning electron microscope (SEM) and a DINS3a atomic force microscope (AFM), respectively. The polar anchoring strength is measured by the 'retardation vs. voltage' method [11], while the azimuthal anchoring strength is measured by using a method of mixing of LC with chiral dopant [12,13]. To study the composition of the treated PI film surface and the chemical bonding characteristics of the PI films, X-ray photoelectron spectroscopy (XPS) is used [14].

3. Results and Discussion

By changing the treating time, we can obtain uniform homogeneous alignment of LCs. The pretilt angle of LC as a function of treating time is plotted in Figure 2. The pretilt angle increases with the treating time and a maximum value of $\sim 15^\circ$ is achieved with treating time of 40 min. The experiment shows that the control of the pretilt angle in a wide range is possible.

To further investigate the mechanism of causing high pretilt angles, we have performed SEM and AFM imaging on the plasma treated PI film surfaces. The nano-scaled clusters are observed by using SEM as shown in Figure 3. After treating 10 min, the cluster structures with groove structure appear obviously. Moreover, the aggregates tend to orientparallel to the ion beam treatment direction. The grooving mechanism, known as the surface morphology effects, seems to be a factor for the LC alignment. Therefore, we investigate that surface roughness by AFM, the root mean square fluctuation of height. The surface roughness without argon plasma beam treatment is 0.177 nm, but changed with the size of aggregation to a range from

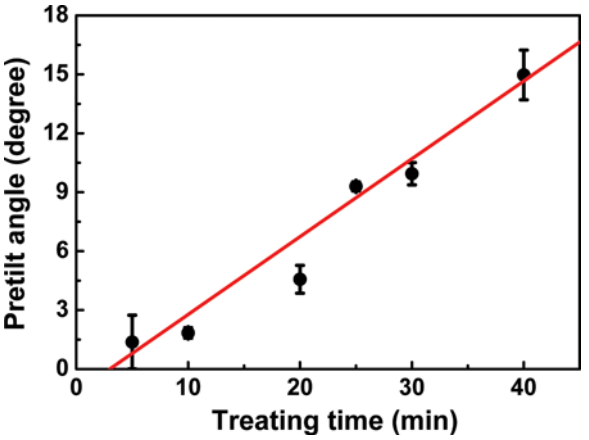

Figure 2. The pretilt angle versus treating time for ion beam. The plasma beam energy is 560 V; the red dotted line is a linear fit. (Figure appears in color online.)

25.56 nm to 70.07 nm with treating time of 40 min as shown in Figure 4. The measured surface roughness is plotted with treating time as shown in Figure 5; it shows a linear proportional relation. Through the results above, it is obvious that the surface morphologies, pretilt angle are correlated.

The plasma beam treating process probably modifies the surface chemical bonds of PI films in favor of LC alignment. The modification of the surface chemical bonds

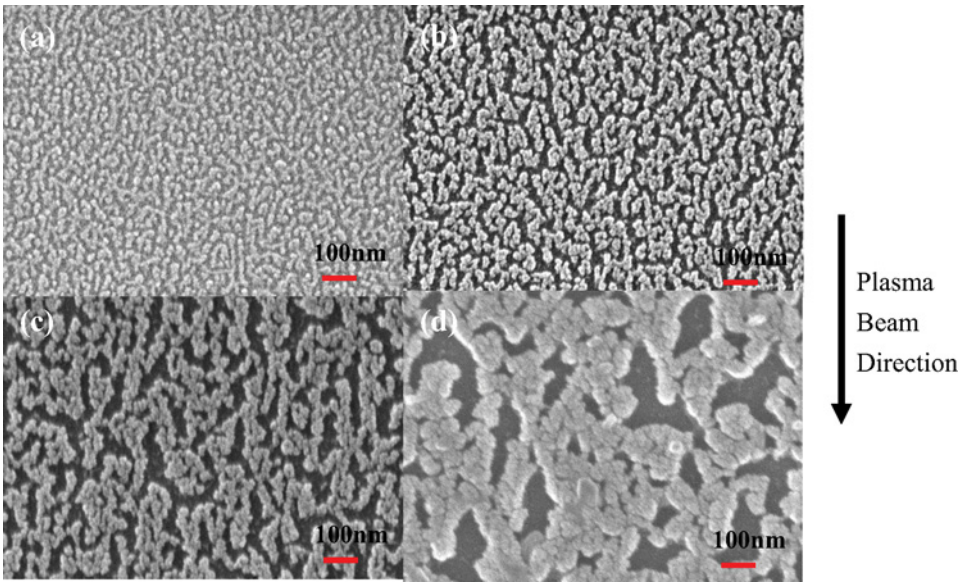

Figure 3. Top view SEM images of PI films treated by Ar plasma beam with different treating times. (a) 5 min, (b) 10 min, (c) 20 min, (d) 40 min. The magnification factor is 100,000×. (Figure appears in color online.)

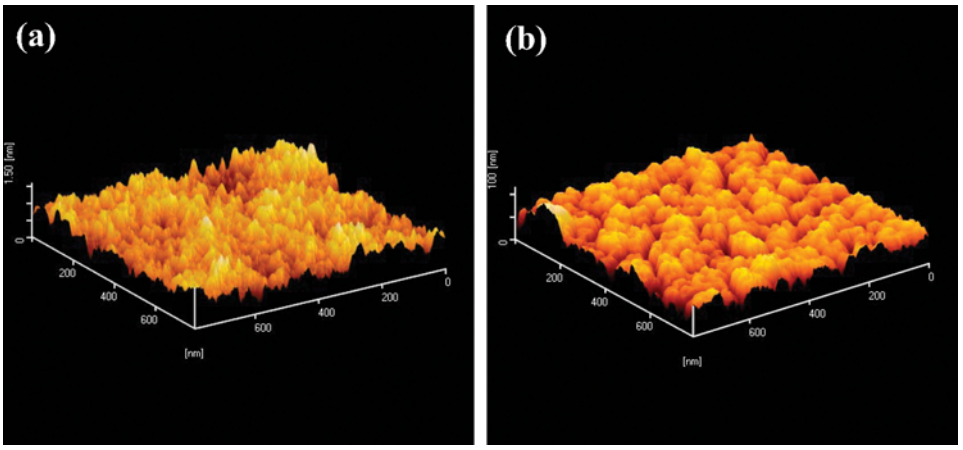

Figure 4. AFM images of PI films in $800 \times 800\,nm^2$: (a) without argon plasma beam treatment that the particle size is about 25.56 nm and (b) after argon plasma beam treated for 40 minutes the particle size is about 70.07 nm. (Figure appears in color online.)

with different treating time is characterized by a series of XPS spectra of C 1 s, Fe 2p and O1 s shown in Figure 6, respectively. All the C 1 s, Fe 2p, and O 1 s spectra are calibrated by shifting the peak position of C 1 s spectra to 284.7 eV that is the energy position of C−C bond. The complex structure of C 1 s includes four components C−C (284.7 eV), C−N (285.68 eV), C−O−C (286.29 eV), and C=O (288.61 eV) for what we are focused on [15]. In Figure 6(a), the small peak at 288.6 eV is recognized as for the C=O bonds in the PI structure, which suddenly decreases as long as argon plasma treating is processed. It indicates that some C=O bonds are broken during argon plasma treatment. The iron atom is also sputtered simultaneously in the sputtering process because of the electrodes made of stainless steel. The broken C=O bond can react with the sputtered iron atom. However, in the sputtering process, most of the iron atoms emitted from target electrode immediately react with the

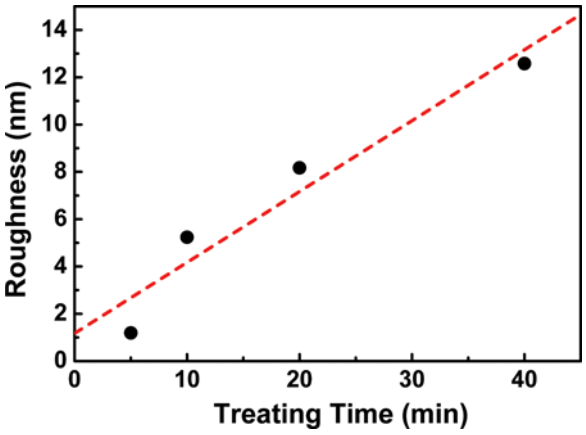

Figure 5. Surface roughness versus plasma beam treating time. (Figure appears in color online.)

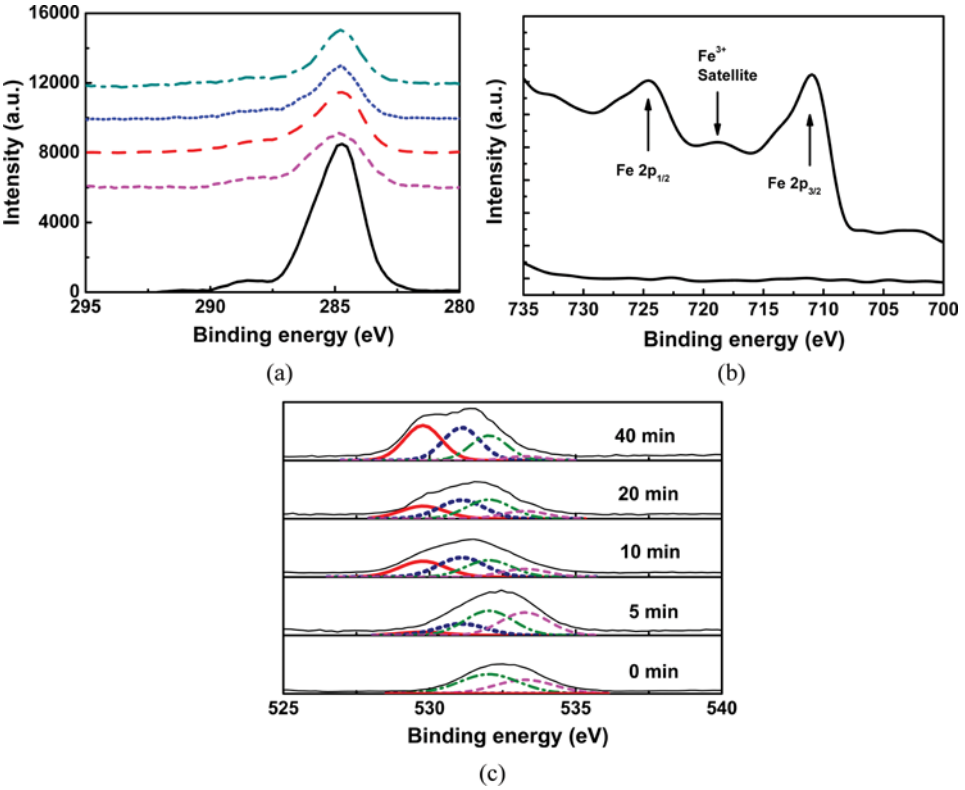

Figure 6. XPS spectra of PI films with various argon plasma treating time for (a) C 1 s and (b) Fe 2p. The O 1 s spectra are deconvoluted into the γ-Fe_2O_3, C−O−Fe, C=O, and C−O−C components (from left to right) as shown in (c). Each curve is labeled by the treating time. (Figure appears in color online.)

residual oxygen in the chamber and then reach the PI film surface as iron oxide. According to the literatures [16,17], the shake-up satellite line at 718.2 eV is a characteristic of Fe^{3+} in Fe_2O_3 as shown in Figure 6(b).

Further, the peak at 710.4 eV of the Fe 2p spectrum indicates that there is no Fe^{2+} iron oxidation state. The film must be composed of the Fe^{3+} oxides, Fe_2O_3 only. On the other hand, only γ-Fe_2O_3 has permanent magnetic moment [18]. As the result, the γ-Fe_2O_3 new component is identified on the treated PI film surface. The rest iron atoms react with PI molecular such as C=O bonds. As shown in Figure 6(c), the O1 s spectra become higher in intensity and the position of peak shifts to lower binding energy after plasma treatment; this indicates that new bonds are generated and re-oxidation process occurs. The structure of O 1 s includes two components, C−O−C (533.26 eV) and C=O (532.03 eV), before plasma treatment. Since the iron atoms are deposited on PI film surfaces and react with PI during plasma treating process. We speculate that bond breaking process occurred and the C=O bonds re-oxidized to C−O−Fe bonds [19]. This speculation of the bond breaking is supported by the decrease of the C=O bonds in the C 1 s spectra. This is reasonable since the polyimide structure is probably either re-oxidized to C−O−Fe bonds after plasma treatment or covered with γ-Fe_2O_3. The formation of C−O−Fe

bonds and γ-Fe_2O_3 will be further justified by the curve-fit of O 1 s that will be described as follows.

Two components C−O−C and C=O in the polyimide structure before plasma treatment and two additional components C−O−Fe and γ-Fe_2O_3 are consistent fits for the O 1 s spectra of the treated PI films, as shown in Figure 6(c). Note that energy positions of C−O−C bonds, C=O bonds, C−O−Fe bonds and γ-Fe_2O_3 are 533.26 eV, 532.03 eV, 531.1 eV and 529.77 eV, respectively. The relative amounts of the four components at different treating time are shown in Figure 7.

The amounts of both C−O−C and C=O bonds decrease with treating time, confirming that the bond breaking process occurs or the bonds are covered by aggregates. Furthermore, the iron-oxide-related bonds increase with treating time. Higher content of C−O−Fe bonds than the γ-Fe_2O_3 bonds indicates that the sputtered ions prefer to react with the PI films rather than the atmospheric oxygen molecules when the treating time is less than 20 min. The content of C−O−Fe bonds seems to have saturated after 10 min treatment. On the other hand, the content of γ-Fe_2O_3 increases with treating time, which is due to the aggregation of nanoparticles evidenced by the AFM measurement as shown in Figure 4. Correspondingly, we speculate that the composition of the groove-like structures on the surface is γ-Fe_2O_3 nanoparticle. In addition, to calculate the area of coverage of nanoscaled clusters is also determined from SEM images and plotted in Figure 8.

The coverage of nanoscaled clusters has a positive tendency with content of γ-Fe_2O_3. As a result, it also supports our assertion that the coated iron oxide films are the particular allotropic form, i.e., γ-Fe_2O_3. In previous work [20,21], a uniform γ-Fe_2O_3 is coated on the ITO substrate can cause a homeotropic alignment of LC. Therefore, we expect that a competition of interaction between the treated PI films and coated maghemite nanoparticles can lead to the resultant pretilt angle.

Using two substrates prepared at same conditions, each LC cell is formed and the polar anchoring strength is measured; Figure 9 shows the relation with treating times. We can see that the polar anchoring strength increases gradually with treating time with similar trend as the pretilt angle. The polar anchoring strength for 5CB is

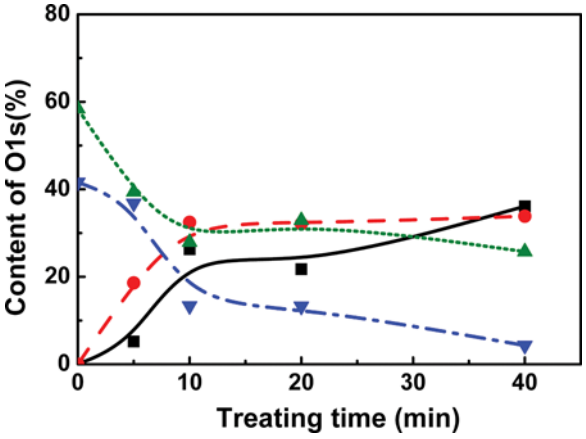

Figure 7. Relative content of the γ-Fe_2O_3 (■), C−O−Fe (●), C=O (▲), and C−O−C (▼) bonds deconvoluted from the O 1 s spectra [Fig. 6(c)] of the PI films with various treating time. (Figure appears in color online.)

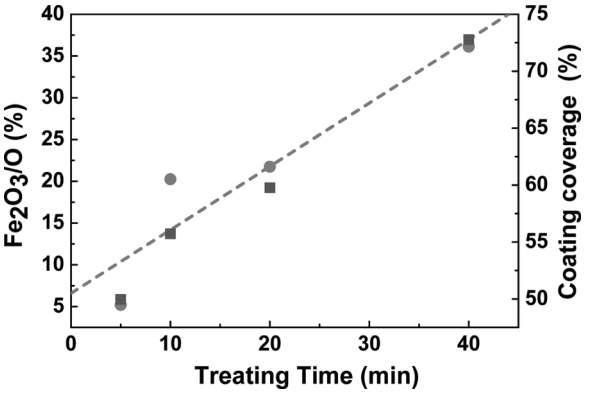

Figure 8. The area of coverage of nanoscaled clusters (squares) and the content of γ-Fe_2O_3 (circles) as a function of the treating time by argon plasma beam.

$1.2 \sim 3.5 \times 10^{-4}\,J/m^2$ by argon plasma beam treatment. On the other hand, the azimuthal anchoring strength for 5CB is $1.73 \times 10^{-5} \sim 3.06 \times 10^{-6}\,J/m^2$ by argon plasma beam treatment. The azimuthal anchoring strength decreases with treating time as shown in Figure 9. For comparison, we have measured the azimuthal anchoring strength for rubbed PI as $2.59 \times 10^{-5}\,J/m^2$. The standard deviation of azimuthal anchoring for samples with treating time less than 10 min are big, which indicates that the alignment is unstable due to the nano-scaled clusters on the surface have not generated the groove-like structures yet. Therefore, we use another method, the twisted cell without chiral dopant, to measure the azimuthal anchoring. The result is about $4.77 \times 10^{-6} \sim 5.81 \times 10^{-7}\,J/m^2$, consistent with that from the method using chiral dopant.

Since the pretilt angle and polar anchoring strength both increase with treating time by argon plasma. We now plot the polar anchoring strength versus pretilt angle relation as shown in Figure 10. They also have a strong positive correlation. Base on

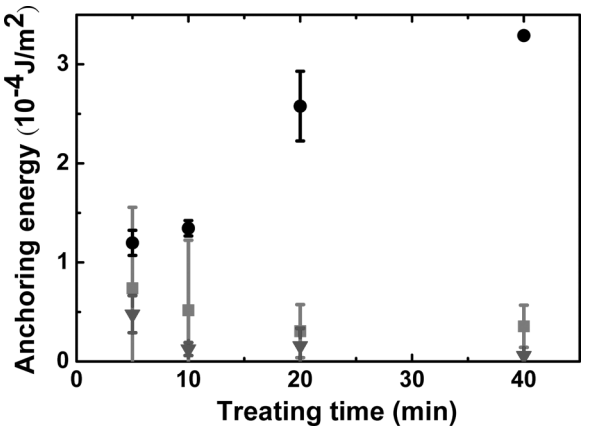

Figure 9. The anchoring strength as a function of the treating time. (●: polar anchoring, ■: azimuthal anchoring by the chiral dopant method, ▼: azimuthal anchoring by the twisted cell method.) The azimuthal anchoring strength is plotted in 10 times of original data.

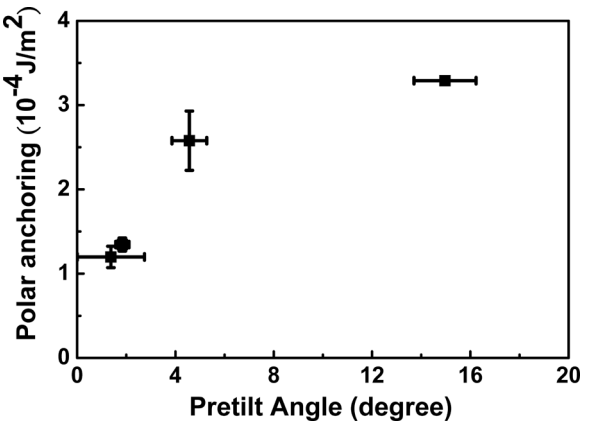

Figure 10. Polar anchoring strength versus the pretilt angle. The plasma beam energy is 560 V.

these results, the γ-Fe_2O_3 aggregation of nanoparticles can dominate the pretilt angle by inducing higher polar anchoring relative to azimuthal anchoring.

4. Conclusions and Perspectives

We demonstrate that coated polyimide substrates after argon plasma treatment with ion energy can obtain reliable alignment for NLCs. The surface is sputtered with γ-Fe_2O_3. The direction of maghemite deposition is anisotropic and parallels to the plasma beam direction in favor of LCs alignment. The polyimide and maghemite nanoparticles in the alignment layer function differently to give variable pretilt angle for LC. The surface roughness of deposited maghemite nanoparticles has the same dependency as pretilt angle to the plasma treating time. The aggregating behavior and the content of maghemite determine the pretilt angle.

Acknowledgment

This work was supported by National Science Council, Republic of China, under grand number 96-2221-E-009-131-MY3 and Academia Sinica AS-98-TP-A10.

References

[1] Greary, J. M., Goodby, J. W., Kmetz, A. R., & Patel, J. S. (1987). *J. Appl. Phys.*, *62*, 4100.
[2] Schadt, M., Schmitt, K., Kozinkov, V., & Chigrinov, V. (1992). *Jpn. J. Appl. Phys.*, *31*, 2155.
[3] Lu, J., Deshpande, S. V., Gulari, E., & Kanicki, J. (1996). *J. Appl. Phys.*, *80*, 5028.
[4] Wu, H. Y., Wang, C. Y., Lin, C. J., Pan, R. P., Lin, S. S., Lee, C. D., & Kou, C. S. (2009). *J. Phys. D: Appl. Phys.*, *42*, 155303.
[5] Stöhr, J.*et al* (2001). *Science*, *292*, 2299.
[6] Chaudhari, P.*et al* (2001). *Nature*, *411*, 56.
[7] Butter, R. S., Waterman, D. R., Lettington, A. H., Ramos, R. T., & Fordham, E. J. (1997). *Thin Solid Films*, *311*, 107–113.

[8] Ahn, H. J., Rho, S. J., Kim, K. C., Kim, J. B., Hwang, B. H., Park, C. J., & Baik, H. K. (2005). *Jpn. J. Appl. Phys.*, *44*, 4092.
[9] Berreman, D. W. (1972). *Phys. Rev. Lett.*, *28*, 1683.
[10] Zhu, H., Lin, Q., & Zhang, B. (2000). *Display*, *21*, 121.
[11] Nastishin, Y. A., Polak, R. D., & Shiyanovskii, S. V. (1999). *Appl. Phys. Lett.*, *75*, 202.
[12] Tang, T. T., Wu, H. Y., Lin, C. J., & Pan, R. P. (2007). *J. Appl. Phys.*, *102*, 063108.
[13] Tang, T. T., Wu, H. Y., Lin, C. J., & Pan, R. P. (2007). *Mol. Cryst. Liq. Cryst.*, *478*, 143.
[14] Briggs, D., & Rivière, J. C. (1990). *Practical Surface Analysis*, Wiley-Chichester.
[15] Ektessabi, A. M., & Hakamata, S. (2000). *Thin Solid Films*, *377*, 621.
[16] Brundle, C. R., Chuang, T. J., & Wandelt, K. (1977). *Surf. Sci.*, *68*, 459.
[17] Gao, Y., & Chambers, S. A. (1997). *J. Cryst. Growth*, *174*, 446.
[18] Cornell, R. M., & Schwertmann, U. (2003). *The Iron Oxides: Structures, Properties, Reactions, Occurrences, and Uses.* 2nd ed., Wiley-VCH.
[19] Wolany, D., Fladung, T., Duda, L., Lee, J. W., Gantenfort, T., Wiedmann, L., & Benninghoven, A. (1999). *Surf. Interface Anal.*, *27*, 609–617.
[20] Wu, H. Y., & Pan, R. P. (2007). *Appl. Phys. Lett.*, *91*, 074102.
[21] Wu, H. Y., Wang, C. C., Pan, R. P., Tang, T. T., Chang, S. J., & Hwang, J. C. (2007). *Mol. Cryst. Liq. Cryst.*, *475*, 45.